VIb1

Losses of cable force at prestressing

Spannungverluste in den Kabeln bei der Vorspannung

Perdas de tensão nos cabos de uma estrutura em betão preesforçado

Pertes de tension dans les câbles d'un ouvrage en béton précontraint

ALLAN BERGFELT
Chief Designing Engineer
Port of Gohtenburg Authority
Gothenburg

One of the most important conditions for calculating prestressed concrete is to have a good knowledge of the different forces which are conveyed into the prestressing cable. To form an opinion of the future existence of the construction it is also necessary to know in which way the forces are going to change after some time.

The cable force at prestressing, checked on the jack or calculated through the extension of the cable is only very exceptionally constant along the length of the cable but changes because of losses of different nature. These losses can be divided as follows: jack losses, losses along the length of the cable, and losses when, and after anchoring the cable. A more accurate division is shown in table 1.

Losses c, μ and k are usually measured by pulling a cable with a jack at one end and checking the force transmitted to the other end. This can be also done by simultaneously measuring the force and the resulting extension of the cable at one end for one loading and unloading cycle. The result given by the first measurement is the total loss, while the second one gives a relation between the final force after losses have taken place and this force's distribution along the cable. These results give an approximate idea of the value of the area of force x cable length. For the determination of the constants for the different losses, this method is scarcely suitable except for cables with comparatively sharp curves. A combination of the different methods will of course give the best results.

TABLE 1

Losses of cable forces in prestressed concrete

Jack losses	$c = c_1 + c_2 + c_3$
Friction in the jack	c_1
Friction at the thread angle for attaching to jack. On the jack	c_2
Friction at the thread angle for attaching to jack. In the anchorage	c_3
Friction losses due to the cable's line shape...	μ
Losses due to deformation of the cable tubes...	k
Friction caused by unintended wave shape	k_1
Adhesion in a compressed tube	k_2
Adhesion or increased friction due to leaking of concrete into the tube	k_3
Losses due to cable slip at anchoring	δ_1
Losses after the anchoring...	$\Delta\sigma$
Creep in the cable steel	$\Delta_1\sigma$
Shrinkage and creeping of concrete	$\Delta_{2,3}\sigma$
Temporary variations such as changes in temperature and load	$\Delta_{4,5}\sigma$

The theory of friction losses at cable curves.

The calculation of friction losses is normally based upon the rope theory. In average structures, curve radii are large enough to justify complete disregard of the effect of the stiffness of prestressed reinforcement.

When a rope is pulled over a curve and bent with the contact angle α, the traction Z is reduced owing to the friction between the rope and the slab (Fig. 1). The contact stress is $p = \frac{Z}{r}$ for a radius r. If the friction coefficient is μ, then the traction Z is reduced of $dZ = \mu\, p\, r.\, d\alpha$ along the length $r.\, d\alpha$

$$\begin{aligned} &\because dZ = \mu\, pr.\, d\alpha = Z.\mu.\, d\alpha \\ &\therefore Z = Z_1.\, e^{-\mu\alpha} \end{aligned} \qquad (1)$$

if α is measured from the end 1, where the force is Z_1.

The variation of length, due to the loading and subsequent unloading to O tension of a curved prestressing cable may be calculated, by means of a simple integration, with this well known formula.

When *loading* from O to P_o the extension is

$$\delta = \int_0^{\alpha} \frac{Z}{EA} \cdot r \cdot d\alpha_x = \frac{Pl}{EA} \cdot \frac{1 - e^{-\mu\alpha}}{\mu\alpha} = \frac{Pl}{EA} \cdot \left[1 - \frac{\mu\alpha}{2} + \frac{(\mu\alpha)^2}{6} - \dots\right] \quad (2)$$

where α is the total angle variation, α_x is the variation up to an arbitrary point and $l = r\,\alpha$. The final form of this expression is obtained by developping $e^{-\mu\alpha}$ in series.

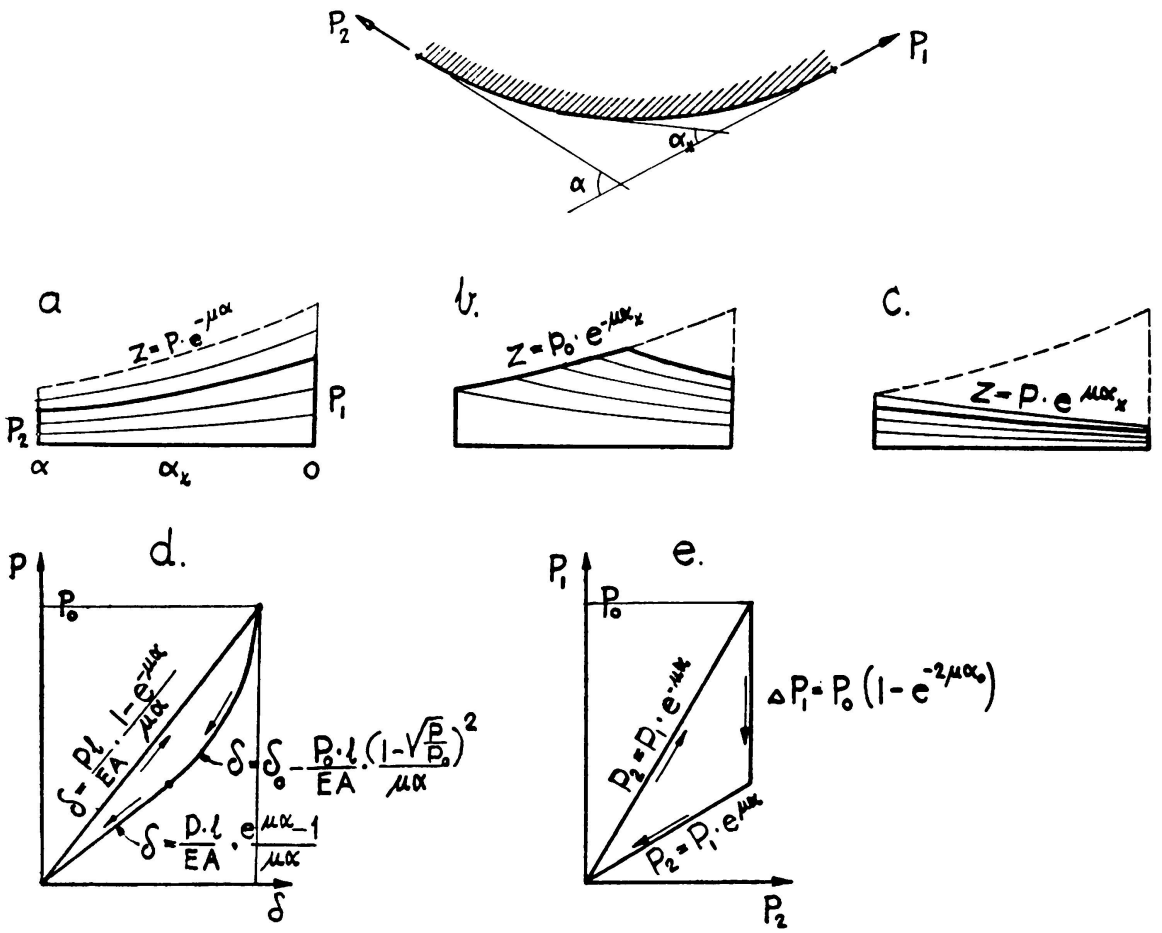

FIG. 1. The theory of friction losses at a cable curve. *a)* Variation of the cable stress along the length of contact. Rope friction. Increasing of the force P_1 from O to P_o. *b)* Discharging from P_o to $P_o \cdot e^{-2\mu\alpha}$. *c)* Further discharging from $P_o \cdot e^{-2\mu\alpha}$ to O. *d)* Relation between stress and strain at the end of the cable curve for one loading and unloading cycle. *e)* Relation between the force P_1 applied at one end of the cable curve and the force P_2 actuating at the other end, for one loading and unloading cycle.

When *unloading*, the theoretical sequence must be divided into two stages. The first one is when the force P is reduced from P_o to $P_o \cdot e^{-2\mu\alpha}$, under which the force at the fixed end will not be reduced. The second stage, is when the force P is reduced from $P_o \cdot e^{-2\mu\alpha}$ to 0, the reduction at the fixed end being proportional.

Calling δ_o the extension due to P_o, the residual extension after the first stage of the unloading is:

$$\delta = \delta_o - \frac{Pl}{EA}\left(1 - \sqrt{\frac{P}{P_o}}\right)^2 = \delta_o - \Delta\delta \tag{3}$$

When changing over to the second unloading stage, i. e. when $P = P_o \cdot e^{-2\mu\alpha}$, the negative term reaches its maximum value

$$\Delta\,\delta_\alpha = \delta_o\,(1 - e^{-\mu\alpha}) \tag{4}$$

Along the second unloading stage, i. e. from $P_o \cdot e^{-2\mu\alpha}$ to 0, the residual extension is:

$$\delta = \frac{Pl}{EA} \cdot \frac{e^{\mu\alpha} - 1}{\mu\alpha} = \frac{Pl}{EA} \cdot \left[1 + \frac{\mu\alpha}{2} + \frac{(\mu\alpha)^2}{6} + \ldots\right] \tag{5}$$

At the change-over point between the two unloading stages the δ curves are tangent to each other and the residual extensions is $\delta = \delta_o \cdot e^{-\mu\alpha}$

It will be noted that, in all the formulae for δ, either r or $l = r.\alpha$ are found, besides α. From this it is seen that the variation of length cannot, as is the case for the friction loss, be independent of the curve's shape.

The above expressions giving a relation between P and δ for one loading and unloading sequence are shown in Fig. 1 - d; Fig. 1 - e shows the relation between the external force P_1 and the force P_2 at the fixed end.

To illustrate the theoretical curves, results of earlier experiments [4] carried out during 1951 and 1952 according to a program drawn up by me, are also shown. This example has been chosen because the prestressing cable, in this case, is curved practically along its whole length and the shape, consequently, corresponds very nearly to the above mentioned theoretical curves.

Fig. 2 shows the dimensions and shape of the prestressing cable and its stress-strain diagram; its main interest lies in the fact that it also shows the measured results under symetrical as well as one sided loading cycles. Under the measured curves are the corresponding theoretically calculated ones for different values of μ. The likely value for μ is, of course, the one which gives the best resemblance between the measured and calculated curves. The theoretical curves are calculated with a probable jack loss of 3 %, i. e. c = 0,97. Experiments made with the press in KTH's Laboratory for Building Statics, have shown losses as small as 1 % for new jacks and as high as 8 % for jacks that have been in use. Experiments at the site, extending two jacks against each other, have shown losses from 1 to 6 %. It follows that 3 % must probably be a reasonable average value.

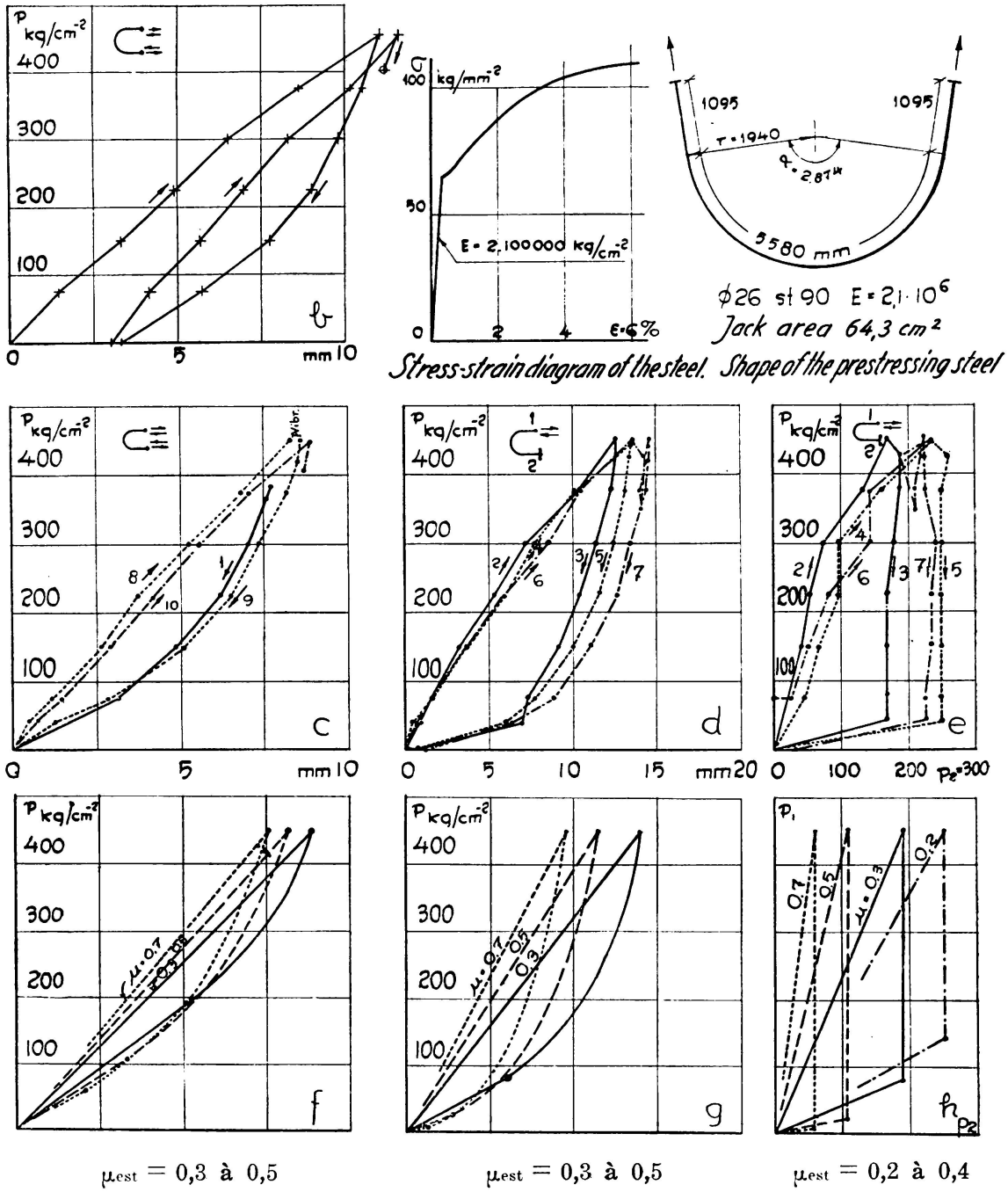

FIG. 2. *Results of tests with prestressed bars of almost semicircular shape* (the Fig. is from the article Ref. 4). *b)* P-δ-diagram at the first loading and subsequent unloading and reloading. Symmetrical tension from both ends. *c)* Repeated loading and unloading according to b. *d)* Repeated loading and unloading at tension from one end. *e)* $P_1 - P_2$-diagram corresponding to d. *f, g, h)* Theoretical curves corresponding to the measured c, d, e. μ_{est} is estimated by comparison between the figures for various presumed μ values.

Any loss k due to unintentional deformation of the cable tubes was in this case, not separately determined but related to μ. The length being small and the steel in the tube stiff, the effect of k ought to be small.

It may be observed in Fig. 2 - b that the first loading gives a far greater extension than the later cycles. This can partly be explained by the fact that in this case, due to the small bending radius, the cable tubes are likely to buckle at the bend causing the formation of folds. When the cable is stretched these folds are pressed down and this deformation appears as an extension of the cable. To a certain extent it is, however, a real extension presumably owing to the fact that the cable at the bend has been loaded above the flow limit, and a levelling by sheer traction gives a greater stretching than normal. The curve corresponding to the first loading is consequently markedly set apart from the following cycles. These also show, however, considerable spreading, which indicates that the value of μ is not wholly fixed. Any marked reduction of μ as the number of loading cycles increases is hardly shown although such a reduction seems obvious.

Experimental results observed during the construction of two bridges.

In 1953 and 1954 two bridges were built for the Port of Gothenburg, over the Rosenlund canal, and a number of measurements were made to determine the prestressing losses and the deformations. Both bridges are freely-supported beam bridges and the main beams are prestressed according to Freyssinet's system, (see Fig. 3).

At the first bridge the measurements were made by determining the force and corresponding cable extension at one cable end only. The determination of he constants gave the results [4] $\mu = 0{,}5$, $c = 0{,}90$ and $k = 65$ kg/m for 26 ton or $k = 0{,}003^1/_m$, which k corresponds to an imagined change of direction of $^1/_2{}^\circ$ per m. Judging among other things, from the shape of the prestressing bars selected for the investigation and from the spreading of the test results, it seems that the sharing of the losses amongst those represented by c and by k is not very accurate.

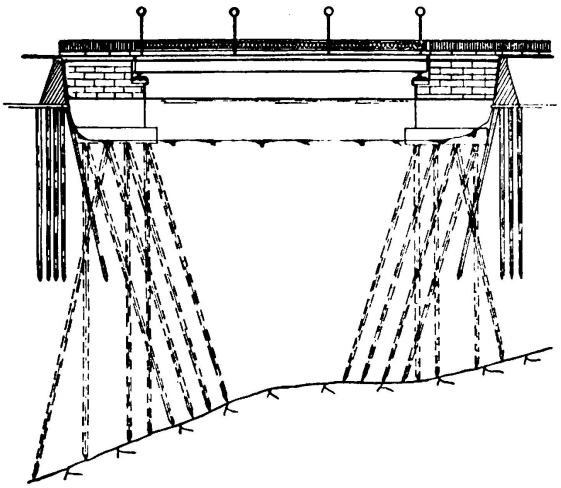

FIG. 3. Bridge over Rosenlund canal, Gothenburg. Span 18,5 m.

During the tests carried out in 1954 in connection with the construction of the other twin bridge, the steel cables were therefore especially selected for testing so that the resulting measurements should allow a separate determination of the different influences. The measurements were, again, carried out so as to include also the determination of the force at the fixed cable end.

Fig. 1 shows the variation curve of the force along a continuous cable bend for a loading and unloading cycle. The shape of the interesting cables in the bridge is, however, the one shown in Fig. 4. By combination

of curve parts similar to those of Fig. 1, it is possible to obtain the curves of Fig. 4.

Jack losses.

Jack losses are measured from the extension of a free cable pulled at both ends through anchor blocks. This system simultaneously allows a control of the modulus of elasticity E.

The jack loss for a Freyssinet-jack is composed of an internal loss due to the relative movements of its different parts and of losses due

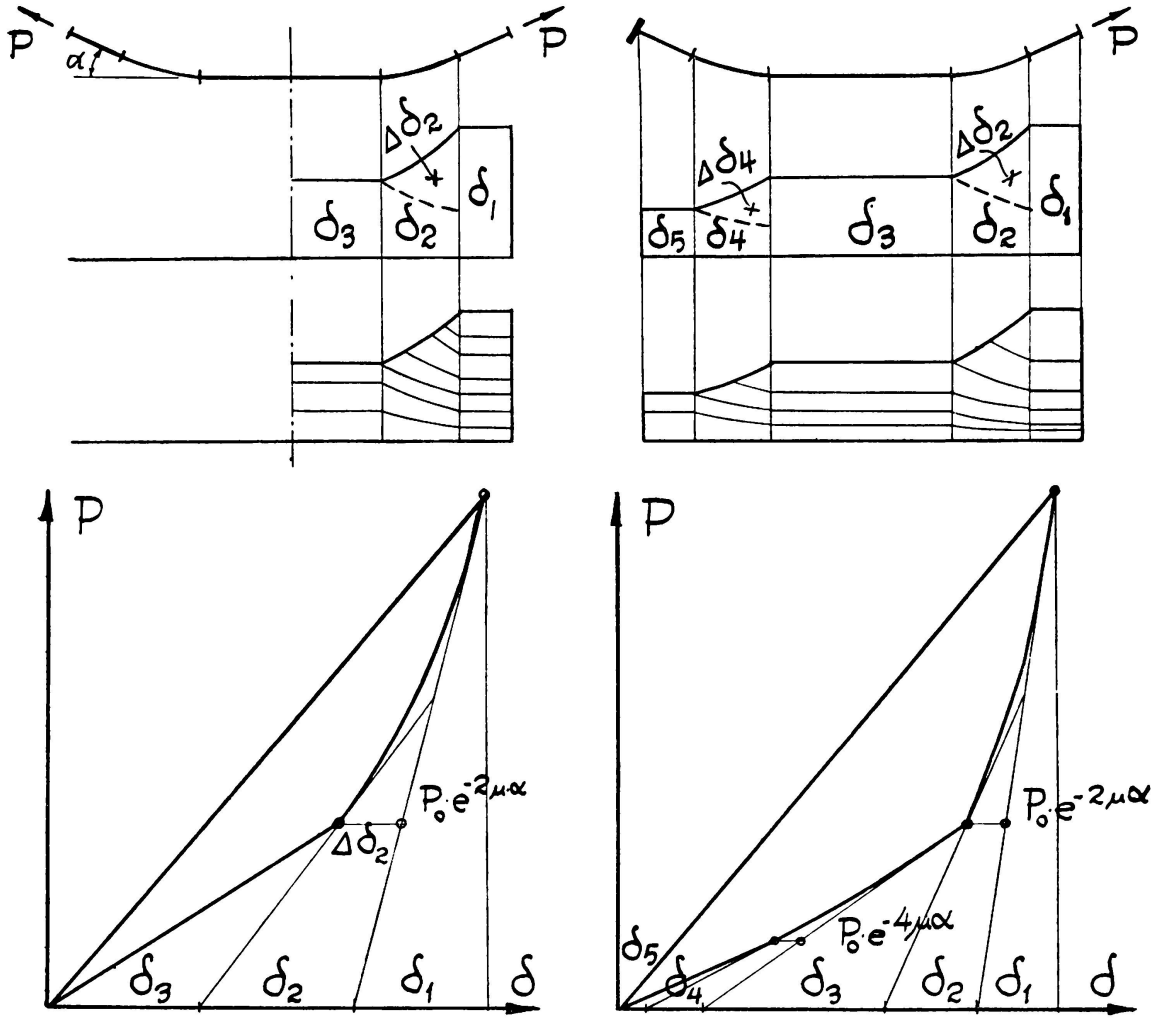

FIG. 4. Curves corresponding to fig. 1 d for cables with straight middle parts.

to the bending of the threads, both at the jack and at the re-bending in the anchor block. Fig. 4 (right) may also show the stretching of a free cable, if it is assumed that the total jack losses are represented by one cable bend.

Fig. 5 - a shows measurement curves for two loading and unloading cycles, jack 1 being the only one operating. Similar curves are obtained

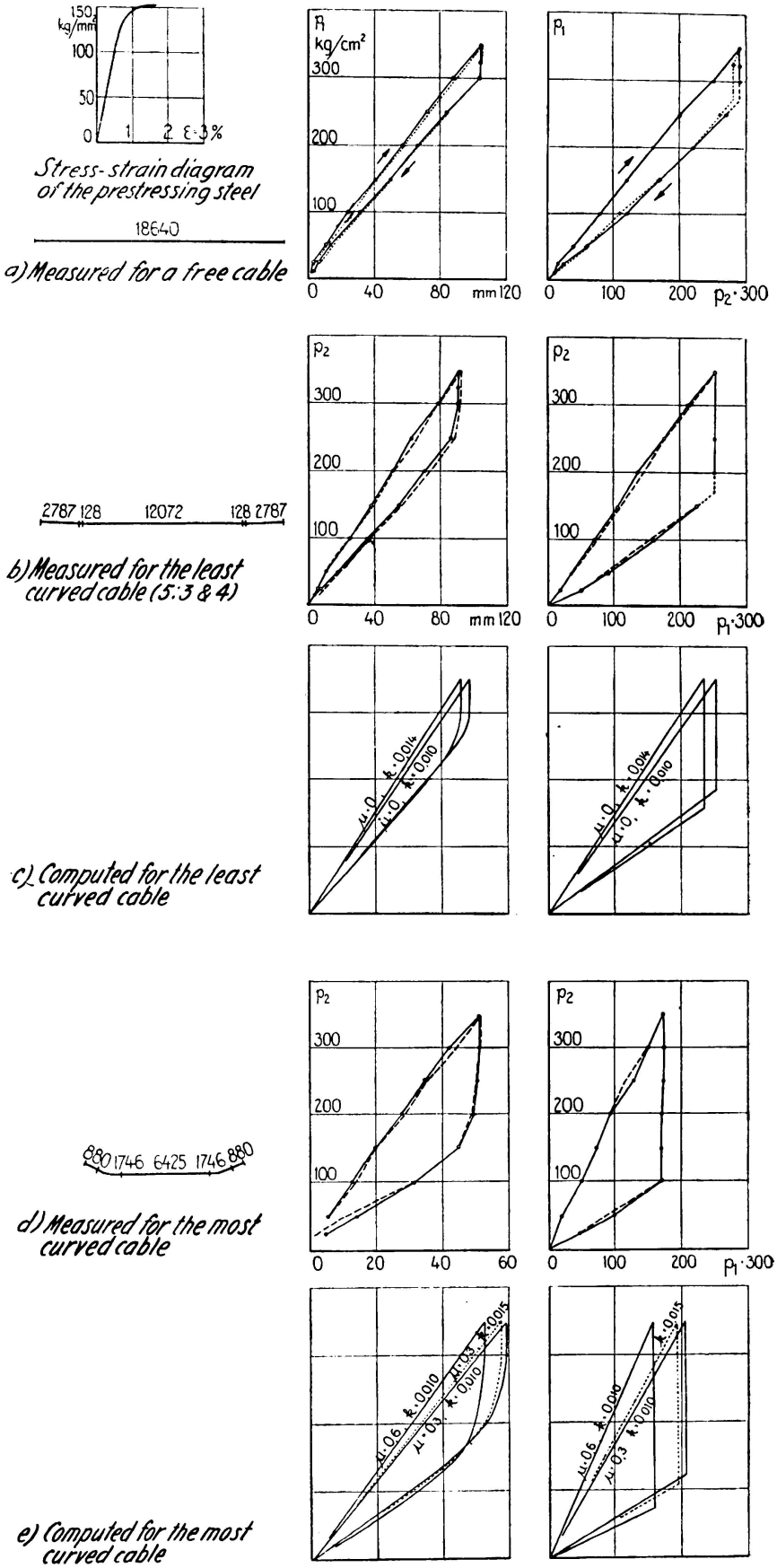

FIG. 5. Measured and theoretically computed p-δ and $p_1 - p_2$ curves of loading and unloading for the different cables.

a) Measured for a free cable.

b) Measured for the least curved cable (5:3 and 4).

c) Computed for the least curved cable.

d) Measured for the most curved cable (5:16 and 13).

e) Computed for the most curved cable.

for jack 2. The cables consist of 12 ø 5,0 mm and the jack's piston area is 81,07 cm².

The curves show fairly regular readings. For $p_1 = 350$at the measured values for both experiments is $p_2 = 290$at, the jack loss in both cases should therefore be $\sqrt{290:350} = 0{,}910$ or 9,0 %. When unloading, the value of p_2 changes first when p_1 is reduced respectively to 272 and 275, and the corresponding losses are $\sqrt{272:290} = 0{,}968$ and $\sqrt{275:280} = 0{,}991$. More satisfactory values of $\sqrt[4]{272:350} = 0{,}939$ and $\sqrt[4]{275:350} = 0{,}941$, are reached if the total jack force, necessary to change the force at the fixed end, is considered for the calculation. The following values are obtained from the diagram corresponding to jack 2,

loading:	$\sqrt{310:350} = 0{,}942$	5,8 %
	$\sqrt{305:350} = 0{,}933$	6,7 %
unloading:	$\sqrt{270:310} = 0{,}933$	6,7 %
	$\sqrt[4]{262:305} = 0{,}927$	7,3 %
total:	$\sqrt[4]{270:350} = 0{,}935$	6,5 %
	$\sqrt{262:750} = 0{,}930$	7,0 %

If all the 12 values are used in order to calculate the average value and mean error, the loss is

$$1 - c = 6{,}2\ \% \pm 0{,}6\ \%$$

Losses can also be determined from the extension diagram shown in Fig. 5. The vertical drop between both curves represents very accurately the double jack loss, as the extension depends mainly on the extension of the straight part of the cable.

The correction, which depends on the camber of the unloading curve, is slight as the camber is only a function of the extension of the jack sections represented in Fig. 4 by $\delta_1 + \delta_2$ and $\delta_4 + \delta_5$. The greatest of these values, i. e. $\delta_1 + \delta_2$ is only about

$$0{,}96 \cdot 350 \cdot 81{,}07 \cdot \frac{665}{2{,}1 \cdot 10^6 \cdot 2{,}35} = 3{,}85\ \text{mm},$$

while the extension of the straight part corresponding to δ_3 is approximately 100 mm.

The values obtained are

c =	$\sqrt{304:350} = 0{,}933$	6,7 %
	$\sqrt{305:350} = 0{,}935$	6,5 %

The values obtained from the diagram corresponding to jack 2 are:

c =	$\sqrt{293:350} = 0{,}916$	8,4 %
	$\sqrt{298:350} = 0{,}923$	7.7 %

The resulting mean value is 7,3 %, which is fairly larger than the one obtained from the proportion between the forces. In the subsequent calculations the assumed likely value is 7,0 %.

A control of E gives in the first experiment

$$E = \frac{Pl}{\delta A} = \frac{0{,}93 \cdot 81{,}07 \cdot 350 \cdot 1864{,}0}{(10{,}8 - 0{,}735) \cdot 2{,}35} = 2\,070\,000 \text{ kg/cm}^2$$

and the corresponding average value is $E = 2{,}05 \cdot 10^6$.

Friction losses owing to unintended wave- shaped cable tubes.

The loss along the cable is assumed to be $e^{-(\mu\alpha + kx)}$, where the exponent's first term is the normal loss due to friction in the curves of the cable. The other term is assumed to depend on the fact that the reinforcement is involuntarily wave-shaped while being erected. The stays cannot be made very tight and, while vibrating the concrete for instance, the cables may happen to be be further displaced. k is calculated here as a constant along the length of the cable x. k could be assumed to be smaller in the bends, where the stays are usually tighter; however, the risk of leakage is perhaps somewhat greater in curves and k in that case ought to be larger.

Experiments have been carried out with the least bent cable for two loading and unloading cycles with p_1 in operation; similar experiments have also been carried out with p_2 in operation. Fig. 5 - b shows two average cycles.

The diagram $p_1 - p_2$ gives the proportion between these forces when loading and unloading as well as the drop corresponding to the change of loading. By comparing Fig. 1 with Fig. 4 it appears that the proportion is $c^2 \cdot e^{-2\mu\alpha} \cdot e^{-kl}$ and the drop the square of this expression. Introducing the different points of the diagram the result will be: loading 242:350 = = 0,720; unloading 168:250 = 0,672; and from the drop $\sqrt{168:350} = 0{,}693$.

A combination of the results also taken from the other experiments gives the following values:

loading	unloading	drop
0,685 0,657	0,768	0,707
0,720 0,720	0,672 0,672	0,693 0,693
0,700 0,685	0,833 0,833	0,755 0,755

If all values are given the same weight, the mean value is 0,723 $\pm$ $\pm$ 0,012.

If the values of the known magnitudes are $c = 0{,}93$, $\alpha = 1°50' = 0{,}032$ radius, and $l = 17{,}9$ m, and if μ is assumed to have probable

limit values, then, for $\mu = 0$, the value $k = 0{,}010$ and for $\mu = 0{,}6$ the value $k = 0{,}008$. The influence of μ in this almost straight cable is thus relatively small and it may be assumed that the likely value of the losses due to the cable's wave shape is

$$k = 0{,}009 \ 1/_m$$

The theoretical curves in Fig. 5 - c, also show that a value of about $k = 0{,}01$ is in agreement with the $p - \delta$ curves.

Friction losses owing to the curves of the cable.

For the most bent cable where the factor $e^{-\mu\alpha}$ dominates, measurements have been carried out, similar to those already described for the least bent one. Two average cycles are shown in Fig. 5-d.

A combination of all the values of p_1/p_2 as given by the diagram of $p_1 - p_2$ gives the following results:

loading	unloading	drop
0,528	(0,303)	(0,378)
0,528	0,572	0,534
0,494	0,588	0,534
0,500	0,588	0,534
0,528	0,572	0,534
0,542	0,572	0,534

If both values within brackets are excluded, the average value is $0{,}542 \pm 0{,}007$. This corresponds to $c^2 . e^{-2\mu\alpha} . e^{-kl}$; introducing $c = 0{,}93$, $\alpha = 25° = 0{,}436$ radius, $k = 0{,}009$, and $l = 11{,}677$ m in the expression, a value $\mu = 0{,}415$ is obtained.

The theoretical curves in Fig. 5-e also show that the pair of values $k = 0{,}010$, $\mu = 0{,}40$ to $0{,}45$ are in agreement with the $p - \delta$ curves. It should be noted that for instance $k = 0{,}020$, $\mu = 0{,}35$ would also be satisfactory but would not suit the straightest cable where even for $\mu = 0$, it would be hardly possible to assume a value higher than $k = 0{,}015$.

Regarding the calculation of the friction losses, it should be noted that the $p_1 - p_2$ diagrams give the total force loss. Calculations based on the rope equation give, in this case, very satisfactory values for different angles. The shape of the $p - \delta$ diagrams give a certain amount of control as to whether or not the distribution along the length of the cable really follows the rope equation. The correspondence of the shapes of the measured curves and the theoretically calculated ones is quite satisfactory. Both experiments described above — one with Dywidag--steel as shown on Fig. 2 and one with Freyssinet-cables as shown on Fig. 5 — give, however, measured diagrams somewhat more «full»

than the calculated ones. The fact that μ at unloading is larger than under normal conditions as long as the load is high possibly explains this difference. For a smaller load, the $p_1 - p_2$ diagrams show that the the value of μ is normal. It may not be entirely impossible to imagine that the particles, pressed hard against the cable tubes, are directed in the direction of the stress. The friction would then have to be quite large to make them return to their original position as long as stress pressure was high.

Cable slip at the anchoring.

When the jack is released and the cable force is transfered to the anchoring, there is a certain slipping of the cable in relation to the anchor block. This will cause a certain reduction of the force in the cable but, as can be seen from Fig. 1 and 4, this generally occurs only

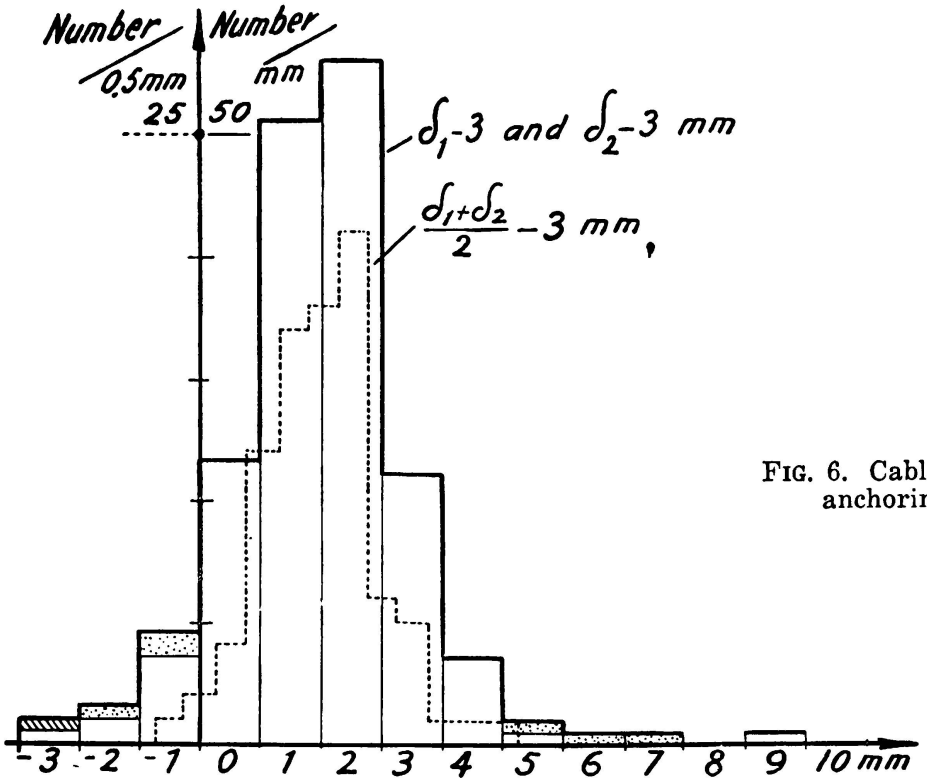

FIG. 6. Cable slip at anchorings.

at the ends. It is however possible, due to the injections for instance, for a certain adjustment of the different forces to occur.

The lock slipping being rather small, as is shown below, its effect is only noticeable in very short cables.

The lock slipping at both ends was measured in both bridges for each one of the 180 cables. The results of these 360 measurements are shown in Fig. 6. In this case the displacement of a point on the cable at a distance of 60 cm from the external surface of the concrete was

measured and reduced by 3 mm corresponding to a shortening of 3,0 to 3,5 mm of the projecting cable end while unloading.

Some results seem to indicate a negative lock slipping. If, however, it is remarked that, in some of the cases, the sliding at the other end of the cable is unusually large, it is obvious that a certain movement of the cable over to one side has taken place. Such pairs of values are marked with dotted areas in the diagram. To eliminate the influence of such effects, the mean value of the readings at both ends of each cable was considered. The corresponding results have been indicated in Fig. 6 with a dotted line. It may be seen that the lock slip is usually 1 or 2 mm. Only in a few cases does this value raise above 3 mm. The mean value is approximately $\delta_1 = 1{,}5$ mm or probably even less if it is considered that the extension of the projecting cable is in some cases as high as 3,5 mm, while for the diagram it is assumed to be 3,0 mm.

Measurement of permanent set.

There is a further alteration of the force in the cable after the anchoring has been carried out, which is principally due to the shrinkage and creep (plastic flow) of the concrete. This is the reason why it is necessary to use relatively high tensile steel with high stresses in order to have sufficient effective stress left, even after the permanent set of the concrete has taken place.

In order to check these losses, the variation of length and bending of the bridge were measured. The measuring began at the same time as the bridge was being prestressed and the resulting diagrams in Fig. 7, show how closely the upward bending follows the stretching of the cables. After a few months, part of the permanent set has already taken place. The diagram also shows that the measured values depend, to some extent upon air temperature changes and upon rain, both of which in combination can give rapid cooling.

Only the main lines of the calculation principle of these deformations are given here. From these deformations it is then possible to deduce the prestressing losses. Secondary influences such as the reduction of the creep due to the decrease of stress in the steel or the influence of the reinforcement upon the shrinkage, are not treated.

Shrinkage and creeping of the concrete.

I have chosen to base the following calculation of the shrinkage and creep of the concrete upon the calculations I had the pleasure of carrying out for I. Häggbom as a complement to his description [5], at the Congress in 1948, of the large concrete arch of Sandö-bridge in Sweden. At the time the transformation of the results obtained from testing upon concrete prisms in the laboratory to the actual arch with its box section of concrete slabs, was undertaken following an idea brought forward in an article by R. W. Carlson [6]. In it he points out the possibility of using an equation corresponding to the heat equation

in order to judge time effect upon shrinkage of concrete objects of different size and form.

The same equation is also valid for electric fields and diffusion of gases; Terzaghi and Fröhlich [7, 8] for instance have also used it for the

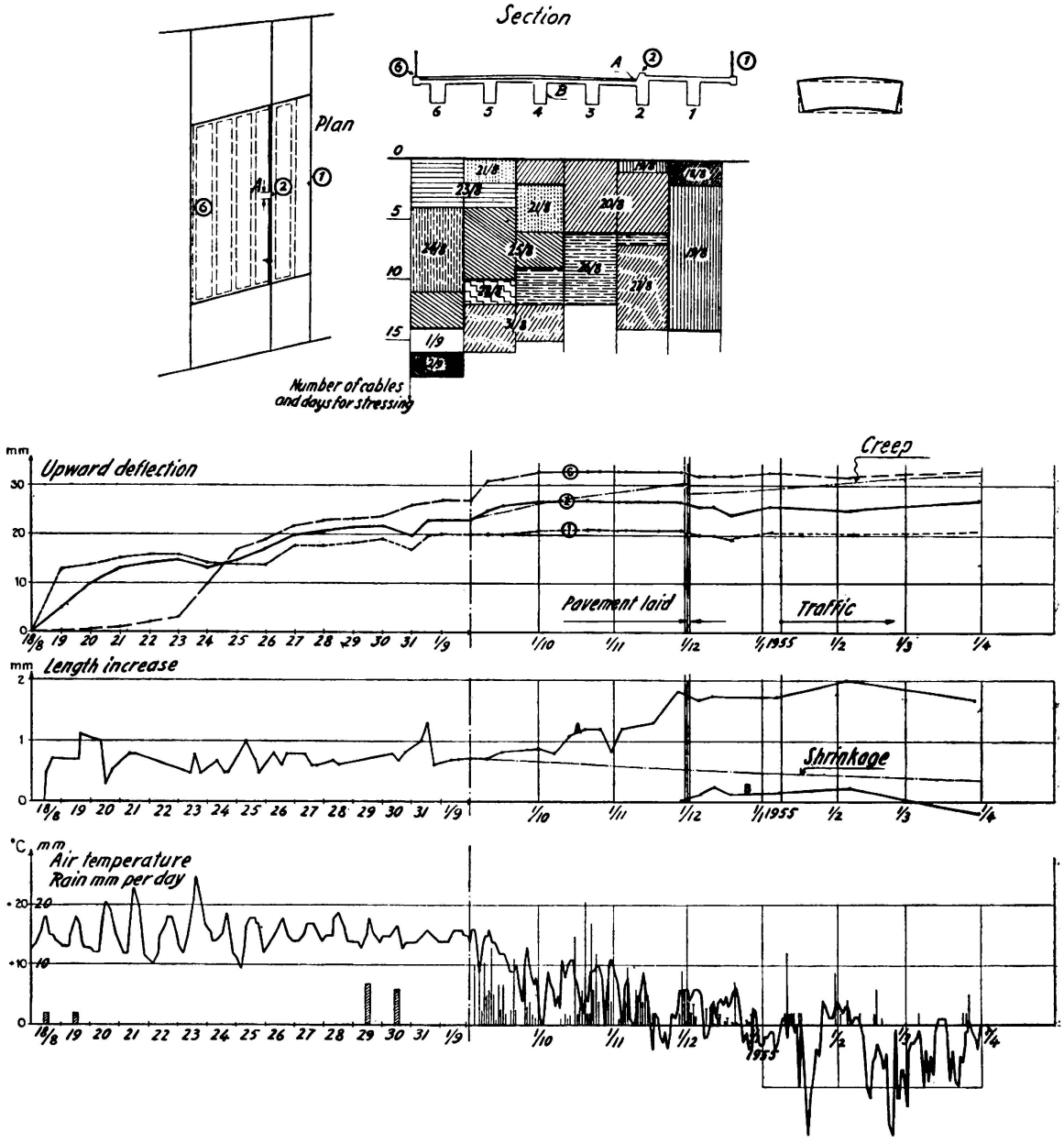

FIG. 7. Days for prestressing of the cables. Deformation – time diagram.

calculation of void water streaming in clay and for the subsequent calculation of the corresponding settling. Because of the strong resemblance existing between that problem and the one treated herewith, the equation is taken in the form given by those authors for parallel plane clay layers.

$$\frac{k}{v\gamma} \cdot \frac{\partial^2 w}{\partial z^2} = \frac{\partial w}{\partial t} \qquad (6)$$

Here, w is the hydrostatic overpressure at a point with coordinate Z, at the time t . k is the water perviousness, v is the specific void water loss, and γ is the volume weight.

For three-dimensional problems, $\frac{\partial^2 w}{\partial z^2}$ has to be changed for the differential parameter of Laplace, $\Delta^2 w$.

The equation is dealt with in detail in different treatises [9, 10] on heat, and reference is only made here to the simple solution valid for hydrostatic pressure wich is sinus-shaped at time $t_o = 0$. After time t has elapsed, it has been uniformly diminished by means of the multiplier $e^{-\beta T}$, where β is a constant and $T = at/d^2$ (7)

in which d is the thickness of the layer and $a = \frac{k}{v\gamma}$. Using the same symbol μ for the time function of settlement, as in the above-mentioned paper [5], one has $\mu = 1 - e^{-\beta T}$.

If the original hydrostatic pressure has a form other than the simple sinus-shape, it can, for instance, be expressed by means of Fourier series, and the solution can be written in a generalized form:

$$\mu = 1 - \Sigma A_n \cdot e^{-\beta_n \cdot T} \tag{8}$$

If instead of a slab one has a long prism, this could then be mathematically treated as being composed of two slabs, one for each direction and, in the case of a square prism the solution is

$$\mu^{pr} = 1 - (\Sigma A_n \cdot e^{-\beta_n \cdot T})^2 \tag{9}$$

The curves for shrinkage K and creep f, wich were measured for the prisms at Sandö and are intended to be used here as it is plausible that the concrete is similar, are given in Fig. 13 of the above- mentioned article [5]. They are easy to express approximately, by means of equation (9) :

$$\mu_K^{pr} = 1 - e^{-8\beta T} \quad , \quad \mu_f^{pr} = 1 - \frac{2}{3} \cdot e^{-\beta T} - \frac{1}{3} \cdot e^{-32\beta T} \tag{10, 11}$$

With t in years, h in cm and, if a is a constant for the concrete used, then constant $\beta \cdot a = 138$ cm^2 year.

This expression is easily made valid for the case of a slab by means of the relation between equations (9) and (8) :

$$\mu_K^{s} = 1 - e^{-4\beta T} \quad , \quad \mu_f^{s} \approx 1 - \frac{4}{5} \cdot e^{-\beta/2 \cdot T} - \frac{1}{5} \cdot e^{-32\beta T} \tag{10-a, 11-a}$$

From this and assuming the shrinkage to be

$$K = \frac{100-R}{100} \cdot k \cdot \mu_K \text{, and the creep to be } f = \sigma \cdot F \cdot \mu_f \qquad (12, 13)$$

where R = relative humidity, $k = 0{,}88 \cdot 10^{-3}$, σ = stresss in kg/cm² and $F = 0{,}94 \cdot 10^{-5}$, the sinking the aforesaid bridge crown was calculated. In the the above-mentioned paper [5] it was seen that calculated and measured sinking were almost exactly the same, 17 cm, 5 years after the crown was built. This corresponds to a theoretical sinking of 28 cm counted from the time, some months earlier, when the watering was ceased and the load brought on. After another 5 years the measured value was 19 cm and the corresponding calculated value was 20 cm. The difference is relatively still less when the theoretical total values 30 and 31 cm are compared. It may also be seen that the values are high up in an extrapolated, and thus very uncertain, part of the μ_f^{pr}-curve.

This extremely good agreement is probably due to a great extent, to the fact that, in this case proof-objects and actual construction have rather similar cross dimensions and about the same load and variation of relative humidity. For more than 20 years it has been pointed out [11] that shrinkage and creep should not be calculated totally independently; this is possibly connected with the very curved shape of the elasticity curve of concrete. It has also been pointed out by G. Pickett [12], that surface resistance should not be neglected in diffusion or heat equations. The above deduction, where no surface resistance has been taken into account, corresponds to a Pickett's factor $B = \infty$, As a matter of fact, $B = 2$ should give a little better agreement if the «diffusion constant» is similarly altered. The difference is, however, extremely slight and it seems possible to choose any value B as long as the other constant is equivalently adopted. It therefore, seems necessary to take B into account only when comparing tests of various dimensions and loadings.

In the case of the Pustervik bridge, the simplified equations (12) and (13), with time functions (10-a) and (11-a), are applied independently of each other for the calculation of camber and length variation.

The time function must be altered for application to bending. In this case, the parts nearest to the surface must, of course, play a most significant part and the creep function for a bended slab will be rather similar to the one for a prism with centric pressure. An estimated curve for the upward bending due to creep where the irregular shape of the slab and the beam were considered, is drawn on Fig. 7 as a thin line.

The length variation at point A due to creep, is composed of compression with its μ_f, and of bending with its faster increasing μ_{fb}; the shrinkage is to be added to both of these. In Fig. 7 only the shrinkage is drawn as a thin line merely in order to give an idea of its magnitude.

It may be seen that there is not as yet good agreement between these uncorrected calculated values and the measurings. The most important influence to be added is presumably the creep of the steel.

Temperature variations.

Temperature variations also have a great influence upon the measurings, in spite of the fact that most of the length variations due to temperature are eliminated by measuring with a steel bar placed under the paving, directly upon the concrete surface. The temperature differences ought therefore to be small and the length variations ought not to differ greatly.

In order to give at least a qualitative picture of the conditions for day and night variation of temperature, some diagrams are included, even though they are primarily established for concrete cisterns and dams where the temperature changes are rather large on one side and small on the other. They are, however, also valid for relative conditions between surface and centre of a rather thick concrete construction or, as in this case, for a bridge deck the upper surface of which is exposed to sun and rain, whilst the conditions underneath are more constant.

Fig. 8 shows the temperature conditions in a concrete wall, one surface of which is exposed to a sinus-shaped temperature change with the amplitude ϑ_{10} and the period T. For an infinitely thick wall the solution [9] is

$$\vartheta = \vartheta_{10} \cdot e^{-kx} \left(\cos \frac{2\pi t}{T} - kx \right) \quad , \quad k = \sqrt{\frac{\pi}{aT}} \tag{14}$$

Here the temperautre conductive power a is $2 \cdot 10^{-3}$ to $3{,}5 \cdot 10^{-3}$ for concrete. In Fig. 8, conditions corresponding to a wall with a thickness d such that kd = 4 are shown; for day and night variation this corresponds, to a 0,5 to 0,6 m thick wall, which is enough for agreement with the above formula.

M. Ritter [13] has given a solution for the case of a wall with a smaller thickness and under the condition that it is the temperature of the surroundings which varies. From this I have calculated the diagrams in Fig. 9 and 10. They show length variations and bending of a slab for sinus-variations of temperature; they also show how the amplitude on the concrete surface is less than that of the surrounding air.

For the actual Pustervik-bridge, no detailed calculations have yet been concluded; it has nevertheless been noticed that the day and night movements, as measured and drawn in Fig. 7, agree in principle with what was to be expected from temperature variations and rain showers.

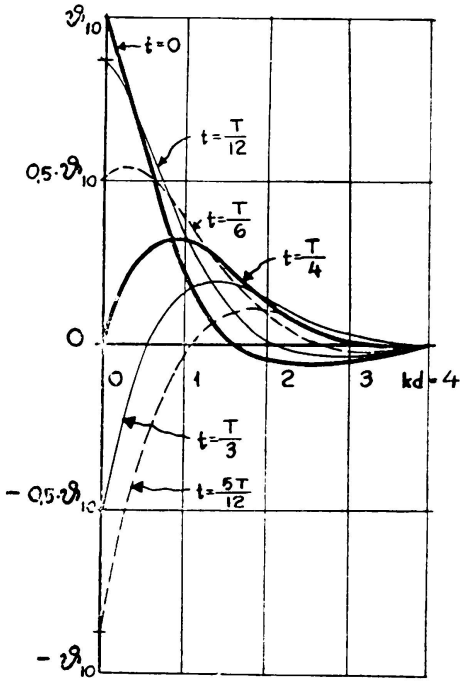

FIG. 8. Temperature conditions for variable surface temperature.

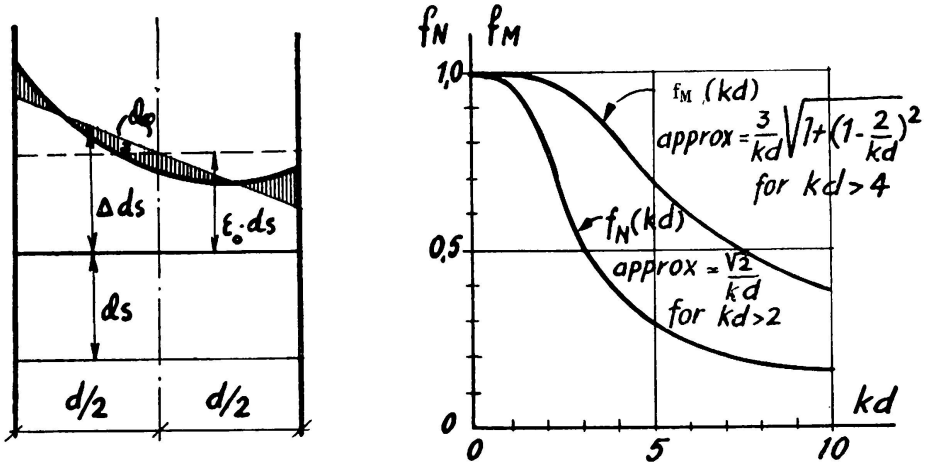

FIG. 9. Length variation and bending of a slab for variable surface temperature. Max. value of the mean temperature $\vartheta_{mo} = \frac{\vartheta_{10} + \vartheta_{20}}{2} \cdot f_N\,(kd)$

Max. value of the bending $\left(\frac{d\varphi}{ds}\right) = \frac{\vartheta_{10} - \vartheta_{20}}{d} \cdot w \cdot f_M\,(kd)$

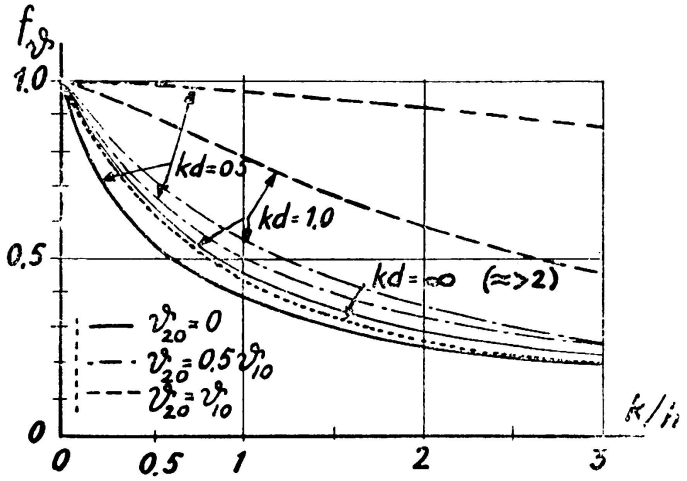

FIG. 10. Amplitude of the surface temperature ϑ_{10} if the amplitude of the surrounding air is ϑ_{ao}

$\vartheta_{10} = \vartheta_{ao} \cdot f_\nu$ Here $f_\nu = f_\nu\left(\frac{k}{h}, kd, \frac{\vartheta_{20}}{\vartheta_{10}}\right)$ where $h = \frac{\alpha}{\lambda}$

and $\alpha = 3$ at calm, $= 10$ for gentle wind and $= 500$ for rain and storm.

BIBLIOGRAPHY

1. GUYON, Y. — *Béton précontraint.* Paris, 1951.
2. LEONHARDT, F. & MÖNNING, E. — *Reibung von Vorspannglidern für Spannbeton.* Beton- und Stahlbetonbau. 1952 H. 2.
3. COOLEY, E. H. — *Research report n.° 1,* Cement and Concrete Association. London, 1953.
4. BERGFELT, A. — *Friction and jack losses in prestressed concrete* – Betong, 1954 – N° 1. Stockholm, 1954. (In Swedish, with an English summary).
5. HÄGGBOM, I. — *The bridges at Sandö.* Publication préliminaire. AIPC Troisième Congrès – Liège, 1948 – page 381 (Fig. 13, 14), page 390.
6. CARLSON, R. W. — *Drying shrinkage of large concrete members.* Journal of American Concrete Institute. Jan.-Febr. 1937, page 327.
7. TERZAGHII, K. & FRÖHLICH, O. K. — *Theorie der Setzung von Tonschichten.* Leipzig & Wien, 1936.

8. FRÖHLICH, O. K. — *Über die angenäherte Berechnung des zeitlichen Verlaufes der Porenwasserströmung in belasteten Tonkörpern und der damit verbundenen Formänderungen.* Mémoires AIPC 1937-38, page 133.
9. GRÖBER, H. — *Die Grundgesetze der Wärmeleitung und des Wämeüberganges.* Berlin, 1921.
10. CARSLAW — *The Mathematical Theory of the Conduction of Heat in Solids.* London, 1921.
11. VOGT, F. — *The effect of shrinkage on the deformation of concrete under sustained loads.* Det Kgl. Norske Videnskab. Selskabs skrifter, 1947, n° 1. Trondheim 1949.
12. PICKETT, G. — *Shrinkage stresses in concrete.* Journal of American Concrete Institute. Jan.-Febr. 1946, pages 165-361.
13. RITTER, M. — *Temperaturverlauf und Wärmespannungen in Mauern bei oscillierenden Aussentemperaturen.* Mémoires AIPC, vol. 7, 1943-44, page 293.

SUMMARY

Prestressing force losses have been calculated and measured for two prestressed concrete bridges in Gothenburg. The bridges were built accordind to the Freyssinet system. The measurements were carried out according to two methods:

— By applying a force with a jack at one end of the cable and measuring the force transmited to the other end.

— By measuring both the force and corresponding extension at one end only, the other end being fixed.

The latter is particularly satisfactory for very curved cables and is applied when only one end is accessible. The combination of both these methods gives a certain control of the distribution of the prestressing force along the cable.

Results of these measurements showed jack losses to be of 6,5 to 7 %, which corresponds to c = 0,93. This not only includes jack losses proper, but also stretching losses at the bending of the threads, both at the jack and in the anchor block.

The friction loss in the cable curves corresponds to $\mu = 0{,}42$ in the expression $e^{-\mu\alpha}$.

The friction losses owing to unintended wave-shaped cable tubes correspond to k = 0,009 in the expression e^{-kx} where "x" is the measured length of the cable, in meters.

A previous measurement [4] had given approximately the same or a little higher μ but a different ratio between "c" and "k".

The slip at anchoring was approximately 1,5 mm and exceeded only very occasionally 3,0 mm.

Measurement of permanent set is being carried on for the purpose of checking the calculation of the corresponding losses of prestressing force. Some basic equations for shrinkage and creep are given. The measurements for the hitherto rather short period of time show little agreement, but this probably is due, partly to certain subsidiary influences such as the irregular shape of the bridge and to the reinforcement, and mainly to the influence of the creeping of the prestressed steel.

ZUSAMMENFASSUNG

Zwei nach dem System Freyssinet vorgespannte Betonbrücken in Göteborg dienten zur Untersuchung der Spannungsverluste. Die Durchführung der beiden Messungen erfolgte teils nach dem üblichen Verfahren, indem eine Kraft mit Hilfe einer Spannvorrichtung am einen Kabelende zur Wirkung gebracht und die übertragene Kraft am andern Ende bestimmt wurde, im andern Fall indem die Spannung und die entsprechende Dehnung nur an einem Ende unter Festhaltung des andern Endes gemessen wurde. Die letztere Methode ist besonders für stark gekrümmte Kabel angebracht und praktisch unumgänglich, wenn nur ein Ende erfasst werden soll. Bei der Kombination beider Verfahren kann die Spannungsverteilung längs des Kabels kontrolliert werden.

Aus den Untersuchungen ergab sich ein Spannpressenverlust von 6,5 bis 7 %, entsprechend einem c-Wert von 0,93. Dieser Verlust umfasst den eigentlichen innern Pressenverlust neben den Streck-Verlusten beim Umbiegen der Drähte am Spannschloss und im Verankerungsblock.

Der Reibungsverlust in den gekrümmten Kabeln entspricht einem μ-Werte von 0,42 für den Ausdruck $e^{-\mu\alpha}$.

Die Reibungsverluste infolge unbeabsichtigter, unregelmässiger Form der Kabelrohre entsprechen einem k-Wert von 0,009 für den Ausdruck e^{-kx} wobei "x" die Kabellänge in m, der Kurve nach gemessen, bedeutet.

Eine frühere Messung [4] ergab angenähert gleiche oder etwas höhere μ-Werte, aber eine andere Proportion "c:k".

Die Verschiebung bei der Verankerung betrug angenähert 1,5 mm und schlug nur gelengentlich bis zu 3 mm aus.

Die Messungen der bleibenden Formänderungen werden weitergeführt mit dem Zweck, die Berechnung der entsprechenden Verluste bei der Vorspannung nachzuprüfen. Einige Grundgleichungen für das Schrumpfen und das Kriechen liegen vor. Die Messungen während der bisherigen kurzen Zeitspanne stimmen mit den Berechnungen schlecht überein; der Grund ist wahrscheinlich bei den Nebeneinflüssen zu suchen, z. B. bei der unregelmässigen Form der Brücke und der Bewehrung, besonders aber beim Einfluss des Kriechens im vorgespannten Stahl.

RESUMO

Mediram-se e calcularam-se as perdas de tensão em duas pontes de betão preesforçado situadas em Gotemburgo. Estas duas obras tinham sido executadas de acordo com sistema Freyssinet.

As medições foram efectuadas por dois métodos diferentes:

— Esticando os cabos com um macaco num dos extremos e medindo a tensão transmitida ao outro.

— Fixando um dos extremos e medindo no outro a força exercida e a extensão resultante.

Este último método dá resultados satisfatórios especialmente no caso de cabos fortemente encurvados e também se emprega quando só uma das extremidades é acessível. A combinação destes dois métodos permite controlar a distribuição da tensão ao longo do cabo.

Os resultados destas medições mostram que as perdas de tensão nos macacos são da ordem de 6,5 a 7 % o que corresponde a $c = 0{,}93$. Este valor compreende, além das perdas devidas aos próprios macacos, as que são causadas pela encurvadura dos cabos no macaco e no cunho de amarração.

As perdas por fricção, devidas à encurvadura do cabo, correspondem a $\mu = 0{,}42$ na expressão $e^{-\mu\alpha}$,

As perdas por fricção, devidas a uma forma ondulada acidental do tubo de protecção do cabo, correspondem a $k = 0{,}009$ na expressão e^{-kx} em que "x" é o comprimento do cabo expresso em metros. Em medições anteriores [4] tinham-se obtido, para μ, valores semelhantes ou ligeiramente superiores; no entanto, a relação entre "c" e "k" era diferente.

O escorregamento nas amarrações era de cerca de 1,5 mm e só raramente ultrapassou 3 mm.

Estão actualmente em curso medições das deformações permanentes que se destinam a verificar as perdas de tensão correspondentes.

O relatório inclui igualmente, algumas equações de base relativas à contracção e à fluência.

Os resultados das medições efectuadas durante o espaço de tempo relativamente curto que medeia desde que as pontes foram postas em tensão não correspondem exactamente aos valores dados pelos cálculos, o que pode talvez ser atribuído em parte a certos factores secundários tais como a forma irregular da ponte, a armadura e principalmente à fluência do aço em tracção.

RÉSUMÉ

Les pertes de tension ont été mesurées et calculées sur deux ponts en béton précontraint situés à Goteborg. Ces deux ouvrages ont été construits selon le système Freyssinet.

Les mesures ont été effectuées suivant deux méthodes différents:

— En tendant les câbles, à l'aide d'un vérin, à l'une de leurs extrémités et en mesurant l'effort transmis à l'autre.

— En fixant l'une des extrémités et en mesurant à l'autre la force exercée et l'extension résultante.

Cette dernière méthode donne des résultats particulièrement satisfaisants dans le cas de câbles à forte courbure et s'applique également quand seule l'une des extrémités est accessible. La combinaison de ces deux méthodes permet de contrôler la distribution de la tension le long du câble.

Les résultats de ces mesures montrent que les pertes de tension aux vérins sont de l'ordre de 6,5 à 7 % ce qui correspond à $c = 0{,}93$. Ce chiffre comprend, non seulement les pertes dues aux verins eux-mêmes,

mais aussi celles dues à la courbure des fils dans le vérin et dans les cônes d'ancrage.

Les pertes par friction dues à la courbure du câble sont données, pour $\mu = 0{,}42$, par l'expression $e^{-\mu\alpha}$.

Les pertes par friction dues à une forme ondulée accidentelle des tubes de protection des câbles sont données, pour $k = 0{,}009$, par l'expression e^{-kx}, où "x" est la longuer mesurée du câble exprimée en mètres. Une mesure antérieure [4] avait donné pour μ des résultats semblables ou légèrement supérieurs, mais le rapport entre "c" et "k" etait alors différent.

Le glissement aux ancrages était de l'ordre de 1,5 mm. et ne dépassait que rarement 3 mm.

Des mesures des déformations permanentes sont en cours dans le but de vérifier les pertes de tension correspondantes.

Le rapport comprend également quelques équations de base relatives au retrait et au fluage.

Les mesures effectuées pendant le temps relativement court qui s'est passé, ne donnent pas encore une correspondance très rigoureuse avec le calcul, ce qui peut, probablement, non seulement être attribué an partie à certaines influences secondaires telles que la forme irrégulière du pont et l'armature, mais surtout à l'influence du fluage de l'acier tendu.